Turevsky, I., Suresh, K., "Efficient Generation of Pareto-Optimal Topologies for Compliance Optimization," International Journal of Numerical Methods in Engineering, Volume 87, Issue 12, pages 1207–1228, 2011

Efficient Generation of Pareto-Optimal Topologies for Compliance Optimization

Inna Turevsky, Krishnan Suresh
Department of Mechanical Engineering
University of Wisconsin – Madison
1513 University Avenue
608-262-3594
suresh@engr.wisc.edu

Abstract

In multi-objective optimization, a design is defined to be *pareto-optimal* if no other design exists that is better with respect to one objective, and as good with respect to other objectives. In this paper, we first show that if a topology is pareto-optimal, then it must satisfy certain properties associated with the *topological sensitivity field*, i.e., no further comparison is necessary. This, in turn, leads to a *deterministic*, i.e., non-stochastic, method for efficiently generating pareto-optimal topologies using the classic fixed-point iteration scheme. The proposed method is illustrated, and compared against SIMP-based methods, through numerical examples. In this paper, the proposed method of generating pareto-optimal topologies is limited to bi-objective optimization, namely compliance-volume and compliance-compliance. Future work will focus on extending the method to non-compliance and higher-dimensional pareto optimization.

Keywords: Multi-objective optimization, pareto-optimal, topology optimization, topological sensitivity.

1. INTRODUCTION

Single-objective topology optimization is now a well established field. Specifically, in continuum mechanics, numerous methods such as homogenization [1], SIMP [2-4] and level-set [5-9], are now capable of solving a large class of single-objective topology optimization problems. Indeed, if a well-defined objective can be articulated, such methods can systematically generate insightful design concepts for complex engineering problems.

However, designers are often faced with conflicting objectives such as cost, aesthetics and performance of a product. Pooling such objectives into a single objective (through some weighted means) is fraught with theoretical and practical difficulties [10, 11]. In such scenarios, one must typically pose and solve multi-objective problems. For example, a relatively simple two-objective topology optimization problem is as follows: "Find the set of topologies with minimal compliance and volume".

Such multi-objective problems do not usually posses a single 'optimal' solution. Instead they exhibit pareto-optimal solutions, where a solution is 'pareto-optimal' if no other solution exists that is better with respect to one objective, and as good with respect to other objectives [12]. Pareto-optimal solutions succinctly address the challenge posed by conflicting objectives [13]. Further, such pareto-optimal designs typically lie on a *pareto-optimal frontier* (see Figure 1) whose computation is also of significant importance.

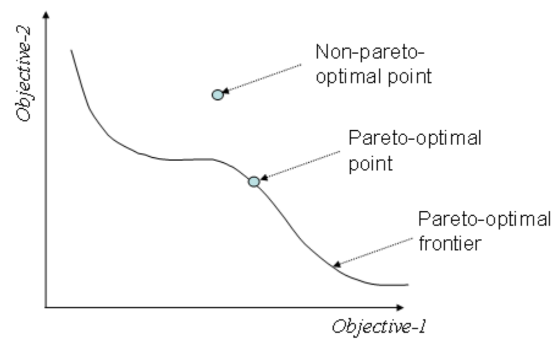

Figure 1: Pareto-optimal points, and pareto-frontier.

Despite the importance of pareto-optimal topologies in continuum mechanics, fundamental questions remain. In this paper, we focus on three of the most important ones identified below.

1. *How does one determine if a given topology is pareto-optimal?*

The definition of pareto-optimality (unfortunately) suggests that a topology is pareto-optimal only if a 'better' topology cannot be found. However, we show here that a topology is pareto-optimal if certain inherent properties associated with the topological sensitivity field are satisfied, i.e., no further comparison to other topologies is necessary.

2. *If a topology is indeed pareto-optimal, what are the local properties of the pareto-frontier at that point?*

While local properties of pareto-frontiers have been addressed in various disciplines [14, 15], it has not found its way into topology optimization. Here, we derive the local properties of the pareto-frontier.

3. *Finally, can one trace the pareto-optimal frontier of a multi-objective topology optimization problem?*

Pareto-tracing are pursued today via genetic algorithms; for example see [16], or by treating the multi-objective problem as single-objective via sequential and weighted-sum optimization methods. We discuss here a deterministic and efficient approach that exploits the pareto-optimal properties mentioned above, together with the fixed-point iteration [17] to generate pareto-optimal topologies.

The remainder of the paper is organized as follows. In Section 2, multi-objective topology optimization is briefly reviewed. In Section 3, we review the concept of topological sensitivity, and establish fundamental results related to pareto-optimal designs. These results are then exploited to propose a new method for tracing pareto-frontiers in topology optimization. In section 4, we propose a method to trace the pareto-frontier for compliance-compliance optimization at a fixed volume. In Section 5, numerical experiments comparing the proposed method against SIMP-based methods are presented, followed by conclusions in Section 6.

2. MULTI-OBJECTIVE TOPOLOGY OPTIMIZATION

There is significant amount of literature on topology optimization (ex: review paper [18]), and multi-objective optimization [10-12, 14, 19]. We focus here on the intersection of the two disciplines. Specifically, we consider the multi-objective topology optimization problem:

$$\begin{aligned} &\underset{\Omega\subset D}{Min}\left\{J_1, J_2, \ldots, J_N\right\} \\ &h(u,\Omega)=0 \\ &g(u,\Omega)\le 0 \end{aligned} \tag{2.1}$$

where:

$$\begin{aligned} &J_i: \text{ Objectives (ex: compliance, volume,...)} \\ &\Omega: \text{ Geometry/topology to be computed} \\ &D: \text{ Region within which the geometry must lie} \\ &u: \text{ The displacement field of elasticity} \\ &h: \text{ Equality constraints} \\ &g: \text{ Inequality constraints} \end{aligned} \tag{2.2}$$

Broadly, there are 3 classes of popular methods for solving Equation (2.1):

1. Sequential optimization
2. Weighted optimization
3. Stochastic/Evolutionary optimization

Other pareto-methods such as normalized normal constraints (NNC) [20] are used extensively in (generic) multi-objective optimization, but have not been applied to multi-objective topology optimization (to the best of author’s knowledge), and are therefore not reviewed here.

2.1 Sequential Optimization

The primary concept in sequential optimization is to modify Equation (2.1) as follows:

$$\begin{aligned}&\underset{\Omega\subset D}{Min}\, J_1\\&J_2 = J_2^0;\ldots;J_N = J_N^0\\&h(u,\Omega)=0\\&g(u,\Omega)\le 0\end{aligned} \tag{2.3}$$

where all objectives except one are fixed at some prescribed (reasonable) value [4, 7, 21]. Then the single objective problem is solved to yield a pareto-optimal design. The process is then repeated for a different choice of constraints, and so on. This is easy to implement, but can be computationally prohibitive since each ‘run’ of a topology optimization itself is often expensive. While sequential optimization provides valuable insights, it is rarely used in large-scale multi-objective optimization.

2.2 Weighted Optimization

In weighted optimization, Equation (2.1) is transformed as follows:

$$\begin{aligned}&\underset{\Omega\subset D}{Min}\, w_1 J_1 + w_2 J_2 + \ldots + w_N J_N\\&h(u,\Omega)=0\\&g(u,\Omega)\le 0\end{aligned} \tag{2.4}$$

where the weights are prescribed *a priori*. By appropriately choosing the weights, a set of pareto-optimal designs are obtained. This method has numerous deficiencies [10, 11], but can be useful if implemented in conjunction with engineering insights [22].

A variation of this method is the ‘compromise formulation’ wherein the weights were supplemented by min and max for each objective function. This was exploited in [13] for finding pareto-optimal topologies with ‘minimal compliance and maximal first eigen-value’.

Yet another variation is the physical programming method where other aspects of the objectives, for example, the range within which it must lie, etc, are taken into account in the formulation [23]. Further, for specific applications, such as compliant mechanisms, other weighted-optimization methods have also been successfully implemented [24].

In summary, weighted-methods are very powerful, but have two inherent limitations: (1) not all pareto-optimal designs can be obtained via suitable weighting, and (2) finding suitable weights is non-trivial [10, 11, 25].

2.3 Stochastic/Evolutionary Optimization

Today, the most popular methods for multi-objective optimization are based on the non-dominated evolutionary or genetic algorithms [19, 26-28].

The underlying principle behind this class of methods (there are numerous variations) is as follows. First, one generates a population of designs. Then, through stochastic methods, typically via genetic coding and mutation, some of the designs are modified. The ‘least-fit’ designs are then eliminated, and the cycle is repeated. Specific examples of such methods for multi-objective topology optimization are reviewed below.

In [26], the authors deal with multi-objective topology optimum design, where the two objectives are minimization of volume and maximum displacement under given loading. Multi-objective evolutionary algorithms are used with Voronoi diagrams serving as a geometric representation.

In [29], the two objectives considered in topology optimization are the minimization of compliance, and maximization of the first eigen-value, with the amount of material to be used serving as a constraint. An additional parameter of penalty-timing is also considered.

3. PARETO-OPTIMAL TOPOLOGIES

One of the objectives of this paper is to develop methods to directly trace the pareto-frontier in multi-objective topology optimization. As a specific example in this section, we consider a two-objective topology optimization problem, where one of the objectives is the compliance, and the other is the volume.

3.1 A Two-Objective Problem

In particular, assume that a structure Ω must lie within a space D, illustrated in Figure 2, of unit volume, and dimensions as shown. The structure Ω is fixed on one edge, and carries a unit-load F on the other end as illustrated; the material properties are E = 1, and $\nu = 0.3$. It is implicitly assumed that, for any structure $\Omega \subseteq D$, the displacement satisfies the elasticity equation [30].

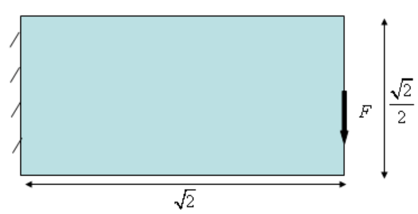

Figure 2: A structural problem on the domain D.

We now define a 2-objective topology optimization problem:

$$\underset{\Omega \subset D}{Min}\left\{J, v = |\Omega|\right\} \tag{3.1}$$

where the first objective is the compliance:

$$J = Fu_F \tag{3.2}$$

(u_F is the displacement at the load-point) and the second objective is simply the volume (or area in 2-D).

Various pareto-optimal solutions exist for Ω. For example, the special case of $\Omega = D$ is illustrated in Figure 3, i.e., where the structure occupies the entire space provided. This is a pareto-optimal design since it is impossible to find a stiffer structure of the same volume.

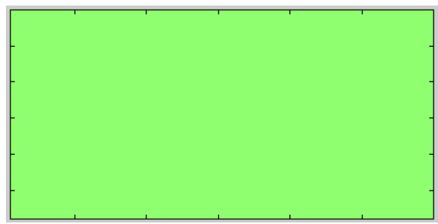

$J = 39; v = 1.0$

Figure 3: A pareto-optimal topology of volume 1.

On the other hand, consider the structures illustrated in Figure 4 (their compliances computed by solving the elasticity equation are also provided). *Are these topologies pareto-optimal* with respect to the objectives in Equation (3.1)? This is fairly hard question that cannot be answered today without either computing the pareto-optimal frontier or searching for 'better' designs.

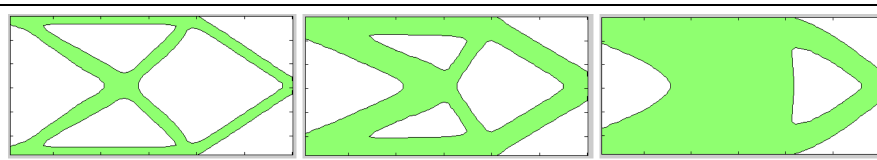

(a) $J = 162; v = 0.3;$ (b) $J = 66; v = 0.5;$ (c) $J = 56; v = 0.65;$

Figure 4: Are these topologies pareto-optimal with respect to Equation (3.1)?

The lack of an 'inherent' test to determine pareto-optimality of topologies in continuum mechanics strongly influences algorithms to generate such topologies. Thus, our first objective is to develop an inherent test. But, first we 'tame' the notion of pareto-optimality since our objective is to trace the frontier.

3.2 Nearby Topologies

It is well known that establishing ‘global minimum’ even for a single-objective optimization problem is hard (except in rare circumstances) [31]. Similarly, establishing *global* pareto-optimality is an open problem; we instead focus here on “local pareto-optimality”.

Towards this end, we introduce the following definition.

Definition 1: Topologies Ω and Ω' are δ-apart if their symmetric volume difference is less than δ, i.e.,

$$\Delta V(\Omega,\Omega') = |\Omega \setminus \Omega'| + |\Omega' \setminus \Omega| \le \delta \tag{3.3}$$

Observe that Equation (3.3) is the sum of the volumes of two set differences. Thus, if Ω is obtained from Ω' by subtracting a disc of volume δ, then $|\Omega \setminus \Omega'| = 0$ and $|\Omega' \setminus \Omega| = \delta$, thus Ω and Ω' are δ-apart. Figure 5 illustrates various topologies that are δ-apart from Figure 4c, where δ denotes the volume of a small disc, shown in Figure 5. Thus, given a volume, nearby-topologies can be constructed by: (a) subtracting or adding a single volume of δ, (b) subtracting or adding 2 volumes of $\delta/2$, (c) subtracting and adding a volume of $\delta/2$, (d) subtracting/adding multiple volumes of δ/N, such that Equation (3.3) is satisfied.

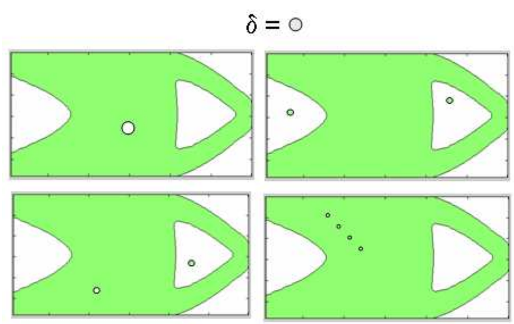

Figure 5: Topologies δ-apart from Figure 4c.

With this notion of nearby-topologies, we now define ‘local’ pareto-optimality by comparing it against other topologies Ω' that are ‘sufficiently close-by’.

Definition 2: A topology Ω is said to be *locally pareto-optimal* if it is pareto-optimal with respect to all topologies that are within a distance δ apart from it, where δ is sufficiently small.

In the next section, we provide necessary and sufficient conditions for a topology to be pareto-optimal. Towards this end, we review the concept of *topological sensitivity* (a.k.a. topological derivative).

3.3 Topological Sensitivity: A Review

The notion of topological derivative has its roots in the seminal paper by Eschenauer, et. al. [32]; this concept has been later explored by numerous authors, for example in [17, 32-39]. The classic ‘subtractive’ topological sensitivity deals with the sensitivity of field problems to subtraction of infinitesimal but arbitrary shaped features, typically discs in 2-D and spheres in 3-D [38]. For simplicity, we assume that the discs/spheres lie in the interior of the domain (see [40, 41] for a treatment of boundary insertion/perturbation). For such shapes, the subtractive topological sensitivity captures the first order impact of inserting a small circular hole within a domain on various quantities of interest [33-39, 42].

For any quantity of interest J, if $B_\varepsilon(p)$ represents a ball of radius ε at point $p \in \Omega$ then the topological sensitivity is defined as the ratio of difference in quantities of interest (with & without hole) to the measure of the hole volume, i.e.,

$$\mathcal{T}^S(p) = \frac{J(\Omega \setminus B_\varepsilon(p)) - J(\Omega)}{|B_\varepsilon(p)|}; p \in \Omega \tag{3.4}$$

where the super-script ‘S’ denotes subtraction. Note that the topological sensitivity is a field since the impact depends on the location of the hole.

For the compliance J in Equation (3.2), the topological sensitivity field in Equation (3.4) simplifies to the following closed-form expression, for 2-D plane-stress problems [43]:

$$\mathcal{T}^S(p) = \frac{4}{1+\nu}\sigma : \varepsilon - \frac{1-3\nu}{1-\nu^2} tr(\sigma) tr(\varepsilon) \tag{3.5}$$

Clearly, Equations(3.4) and (3.5) are only valid where there is material.

Equation (3.5) states that, once the stress and strain are determined for a given structural problem, the change in compliance due to insertion of a hole of area δ at any point p is given by:

$$\Delta J = \mathcal{T}^S(p)\delta + o(\delta) \tag{3.6}$$

where, by definition:

$$\lim_{\delta \to 0} \frac{o(\delta)}{\delta} \to 0 \tag{3.7}$$

In parallel, one can also consider the case of material addition and its impact on the compliance. It is implicitly assumed here that the region $D - \Omega$ is modeled using a soft-material with $E_\varepsilon \ll 1$; such soft-modeling is essential in topology optimization to avoid singularities.

Analogous to Equation (3.4), one can define the topological sensitivity to addition of material:

$$\mathcal{T}^{A}(q) = \frac{J(\Omega \cup B_{\varepsilon}(q)) - J(\Omega)}{|B_{\varepsilon}(q)|}; q \in D - \Omega \tag{3.8}$$

where the super-script ‘A’ denotes addition. For the compliance J in Equation (3.2), similar to Equation (3.5), one can show that the topological sensitivity, for 2-D plane stress problems, with respect to material addition simplifies to [44]:

$$\mathcal{T}^{A}(p) = -\frac{4}{3-\upsilon}\sigma : \varepsilon - \frac{1-3\upsilon}{(1+\upsilon)(3-\upsilon)} tr(\sigma) tr(\varepsilon) \tag{3.9}$$

$\mathcal{T}^{A}(p)$ captures the first order impact of adding a small circular material in the soft-region on the compliance.

Since subtracting/adding material always increases/ decreases compliance, we have, for any pair of points $p \in \Omega$ and $q \in D - \Omega$:

$$J(\Omega \setminus B_{\varepsilon}(p)) > J(\Omega) > J(\Omega \cup B_{\varepsilon}(q)) \tag{3.10}$$

i.e.,

$$\frac{J(\Omega \setminus B_{\varepsilon}(p)) - J(\Omega)}{|B_{\varepsilon}(p)|} > 0 > \frac{J(\Omega \cup B_{\varepsilon}(q)) - J(\Omega)}{|B_{\varepsilon}(q)|} \tag{3.11}$$

Thus, from the definitions in Equations (3.4) and (3.8):

$$\mathcal{T}^{S}(p) > 0 > \mathcal{T}^{A}(q), \forall p \in \Omega, \forall q \in D - \Omega \tag{3.12}$$

The above equation is fairly important in this paper, and we therefore introduce a definition to be employed later.

Definition 3: A pair of fields $(\mathcal{T}^{S}, \mathcal{T}^{A})$ is said to be topologically valid if Equation (3.12) is satisfied, i.e., if:

$$\min(\mathcal{T}^{S}) > 0 > \max(\mathcal{T}^{A}) \tag{3.13}$$

♦

Given a pair of valid topological fields, one can compute the corresponding Ω by considering the level-set:

$$\Omega = \{p \in D \mid \mathcal{T}^{S}(p) > l\} \equiv L(\mathcal{T}, l) \tag{3.14}$$

where the parameter l is so chosen such that the desired volume is achieved, i.e.,

$$|\Omega| = v \tag{3.15}$$

The stresses & strains are related through E in Equation (3.5), and through E_ε in Equation (3.9).

For the structure in Figure 4b, the topological sensitivity field is illustrated in Figure 6, with typical values as shown.

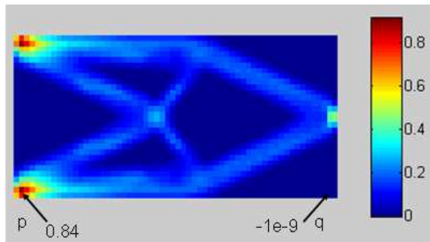

Figure 6: The topological sensitivity field for compliance for the topology in Figure 4.

From Figure 6, observe that:

- If a disc of volume δ is subtracted at the denoted point p, the compliance will change by $\Delta J = 0.84(\delta) = 0.84\delta$, i.e., removing material at p will increase the compliance (make the structure softer) by a significant amount.
- If material of volume δ is added at the denoted point q, then the compliance will change by $\Delta J = -10^{-9}\delta$, i.e., adding material at q will decrease the compliance (make the structure stiffer) but only slightly.

3.4 Local Pareto-Optimality

We now state and prove the main claim on local pareto-optimality by exploiting the topological sensitivity fields.

Lemma 1: A necessary condition for a domain Ω to be locally pareto-optimal with respect to Equation (3.1) is that its topological sensitivity fields must satisfy the inequality:

$$\min(\mathcal{T}^S) + \min(\mathcal{T}^A) \geq 0 \tag{3.16}$$

Proof: Let Ω' be a nearby topology with *identical* volume at a distance of δ from it, i.e., Ω' is constructed from Ω by subtracting M discs of radii $\delta_i^S > 0$, and adding N discs of radii $\delta_j^A > 0$, i.e.,

$$\Omega' = \Omega \setminus \sum_{i=1}^{M} B_{\delta_i^S}(p_i) \cup \sum_{j=1}^{N} B_{\delta_j^A}(q_j) \tag{3.17}$$

such that:

$$\sum_{i=1}^{M} \delta_i^S = \sum_{j=1}^{N} \delta_j^A = \delta / 2 \tag{3.18}$$

Note that the change in compliance is:

$$\Delta J = \sum_{i=1}^{N} \mathcal{T}^S(p_i)\delta_i^S + \sum_{j=1}^{M} \mathcal{T}^A(q_j)\delta_j^A + o(\delta) \tag{3.19}$$

If Ω is locally pareto-optimal, Ω' cannot have a lower compliance implying:

$$\Delta J = \sum_{i=1}^{N} \mathcal{T}^S(p_i)\delta_i^S + \sum_{i=1}^{N} \mathcal{T}^A(q_j)\delta_j^A + o(\delta) \ge 0, \forall p_i, q_i, \delta_i^S, \delta_j^A \tag{3.20}$$

As a particular choice subtract material of volume $\delta/2$ at a location where $\mathcal{T}^S$ takes a minimum, and add material of volume $\delta/2$ at a location where $\mathcal{T}^A$ also takes a minimum, i.e.,

$$\Delta J = \min(\mathcal{T}^S)\delta/2 + \min(\mathcal{T}^A)\delta/2 + o(\delta) \ge 0 \tag{3.21}$$

In the limit of $\delta \to 0$, from Equation (3.7)

$$\min(\mathcal{T}^S) + \min(\mathcal{T}^A) \ge 0$$

♦

Thus, to determine if a topology Ω satisfies the necessary condition to be locally pareto-optimal, one must:

1. Solve the elasticity problem for $u, \varepsilon \,\&\, \sigma$ over D
2. Compute the topological sensitivity fields per Equations (3.5) and (3.9).
3. Check if Equation (3.16) is satisfied.

Indeed, from the above inherent test, one can easily determine that the topologies in Figure 4a and Figure 4c are *not* locally pareto-optimal. However, the topology in Figure 4b indeed satisfies the necessary condition for local pareto-optimality. In theory, second order checks are necessary to ensure local minimum. However, in practice, we found that the algorithms based on the above Lemma, trace the local minima.

3.5 Pareto-Optimal Topologies

We now use the above result to arrive at an algorithm for tracing pareto-optimal topologies. In particular, let Ω be a locally pareto-optimal topology. The objective is to compute a nearby pareto-optimal topology Ω' whose volume is less than that of Ω by Δv, i.e.,

$$|\Omega'| = |\Omega| - \Delta v \tag{3.22}$$

We rely on a fixed-iteration scheme similar to the ones discussed in [17, 45] in that: (1) given a domain Ω one can compute its topological field, and (2) given a valid topological field, one can compute the corresponding Ω from Equation (3.14). Further, by imposing the above termination criteria for local pareto-optimality, we arrive at the following algorithm.

$$
\begin{aligned}
&\textit{Given}: \text{A pareto-optimal topology } \Omega,\ \text{step size } \Delta v \\
&\textit{Find}: \text{A near-by pareto-optimal topology } \Omega' \\
&\qquad \text{such that}: |\Omega'| = |\Omega| - \Delta v \\
&v' \leftarrow |\Omega| - \Delta v \\
&\Omega' \leftarrow \Omega \\
&\text{Do} \\
&\quad \mathcal{T} \equiv \left(\mathcal{T}^S, \mathcal{T}^A\right) \leftarrow \mathcal{T}(\Omega') \\
&\quad l \ \leftarrow \ |L(\mathcal{T}, l)| = v' \\
&\quad \Omega' \leftarrow L(\mathcal{T}, l) \\
&\text{While } (\mathcal{T}^S_{\min} < \mathcal{T}^A_{\max}) \,|\, (\mathcal{T}^S_{\min} + \mathcal{T}^A_{\min} < 0)
\end{aligned}
$$

Algorithm 1: Finding a pareto-optimal topology with volume decrement of Δv.

The *existence* of the parameter l in the above algorithm hinges on the *existence* of a pareto-optimal domain Ω' satisfying Equation (3.22). If Ω' exists, then its topological sensitivity pair exists and can be computed. Since this pair satisfies Equation (3.12), there exists an l satisfying:

$$\mathcal{T}^S > l > \mathcal{T}^A \tag{3.23}$$

Existence does not imply that the algorithm will converge! Indeed, if a very large step-size is taken for Δv, the algorithm may never converge. In practice, $\Delta v \le 0.1$ is recommended.

To further optimize the step-size Δv, one can estimate the change in compliance at each step. Further, since $\Omega = D$ is pareto-optimal, we have the following algorithm to trace the pareto-optimal curve.

Given : A domain D, Δv
Find : Pareto-Optimal Topologies (J, v)
$\Omega \leftarrow D$
$v \leftarrow |D|$
Do
  $\mathcal{T} \equiv \left(\mathcal{T}^S, \mathcal{T}^A\right)$
  $\Omega \leftarrow$ Algorithm-1$(\Omega, \Delta v)$
  $v \leftarrow v - \Delta v$
While $(v > 0)$

Algorithm 2: Tracing the pareto-optimal curve.

The strength and weakness of the proposed algorithm is that it moves from one local minimum to the next closest local minimum (with a new set of volume constraints) on the pareto-optimal curve. By exploiting the closeness of locally pareto-optimal solutions (as defined in the paper), the computational expense of pareto-tracing is reduced dramatically, as demonstrated via numerical experiments. The short-coming is that a 'far away' and alternate pareto-optimal solution cannot be detected via the proposed method.

4. COMPLIANCE-COMPLIANCE OBJECTIVE

Thus far, the paper focused on two-objective problems where one of the objectives was the volume. Now consider the two-objective problem:

$$\begin{aligned} &\underset{\Omega \subset D}{Min}\{J_1, J_2\} \\ &|\Omega| = v_0 \end{aligned} \tag{4.1}$$

where the volume is constrained, and the two objectives are the two compliances associated with two loads, F_1 and F_2; see Figure 7. Although only one of the loads will be applied at any instant, it is not known *a priori*, which of the two loads will be applied. Thus, the goal is to find a topology of a given volume fraction, that is stiff with respect to both loads … a pareto-optimal problem.

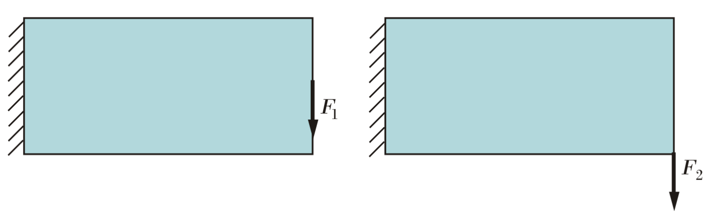

Figure 7: Two load cases, F_1 and F_2

Note each objective has its own topological sensitivity field. For such problems, it is possible to show (using the methods of the previous Section), that a domain Ω is locally pareto-optimal if and only if:

$$\forall p \in \Omega, \forall q \in D-\Omega, \text{ such that } \mathcal{T}_1^S(p)+\mathcal{T}_1^A(q)=0 \tag{4.2}$$

$$\mathcal{T}_2^S(p)+\mathcal{T}_2^A(q)\geq 0 \tag{4.3}$$

i.e., it is impossible to find a nearby topology with identical volume and compliance J_1, but lower compliance J_2. This can be simplified into a single condition:

$$\begin{aligned}&\forall p \in \Omega, \forall q \in D-\Omega\\&\mathcal{T}^S(p)+\mathcal{T}^A(q)\geq 0\end{aligned} \tag{4.4}$$

where

$$\begin{aligned}\mathcal{T}^S &= w_1^2\mathcal{T}_1^S + w_2^2\mathcal{T}_2^S\\ \mathcal{T}^A &= w_1^2\mathcal{T}_1^A + w_2^2\mathcal{T}_2^A\\ w_1 &> 0, w_2 > 0\end{aligned} \tag{4.5}$$

leading to:

$$\min(\mathcal{T}^S)+\min(\mathcal{T}^A)\geq 0 \tag{4.6}$$

Here weights, w_1 and w_2 represent, for example, the likelihood of load F_1 or F_2 being applied. Observe that Equation (4.6) is a generalization of Equation (3.16).

We now use the above result to arrive at an algorithm for tracing pareto-optimal topologies. In particular, let Ω be a locally pareto-optimal topology when $w_1=0, w_2=1$. The objective is to compute a nearby pareto-optimal topology Ω' with identical volume and modified load preference, i.e.,

$$\begin{aligned}w_1^{new} &= w_1+\Delta w\\ w_2^{new} &= 1-w_1\end{aligned} \tag{4.7}$$

We have the following algorithm to trace the pareto-optimal curve.

$$
\begin{aligned}
&\textit{Given}: \text{A domain } D,\ v_0,\ \text{step weight } \Delta w \\
&\textit{Find}: \text{Pareto-Optimal } \Omega \text{ for } (J_1, J_2) \\
&\qquad \text{such that}: |\Omega| = v_0 \\
&\Omega \leftarrow \text{Algorithm-2}(\Omega, \Delta v, w_1 = 0, w_2 = 1) \\
&\text{Do} \\
&\quad w_1 \leftarrow w_1 + \Delta w \\
&\quad w_2 \leftarrow (1 - w_1) \\
&\quad \text{Do} \\
&\qquad \mathcal{T} \equiv \left(w_1^2 \mathcal{T}_1^S + w_2^2\, \mathcal{T}_2^S, w_1^2\, \mathcal{T}_1^A + w_2^2\, \mathcal{T}_2^A \right) \\
&\qquad l \ \leftarrow \ |L(\mathcal{T}, l)| = v \\
&\qquad \Omega \leftarrow L(\mathcal{T}, l) \\
&\quad \text{While } (\mathcal{T}_{\min}^S < \mathcal{T}_{\max}^A) \,|\, (\mathcal{T}_{\min}^S + \mathcal{T}_{\min}^A < 0) \\
&\text{While } (w_1 < 1)
\end{aligned}
$$

Algorithm 3: Tracing the pareto-optimal curve for $J_1 - J_2$.

The strength of the proposed algorithm is that it moves from one load preference to the next without returning to the initial design domain D.

5. NUMERICAL EXPERIMENTS

In this Section, we illustrate the results from Sections 3 and 4 through numerical experiments. Unless otherwise stated, for all the experiments below, the default parameters for the proposed algorithm are as follows:

- We trace the pareto-optimal curve starting from $v = 1$ to $v = 0.5$ in 10 steps, i.e., $\Delta v = 0.05$.
- The domain D is discretized into (60,30) linear quad elements.
- We use a Gaussian filter of radius 0.8 to smoothen the topological sensitivity field. This is similar to the use of filters in SIMP [4].

For SIMP, we use the Matlab code described in [4] with the following parameters:

- For each volume fraction v, we determine the optimal topology by minimizing compliance (i.e., single objective minimization).
- The domain is again discretized into (60,30) linear quad elements.
- We use a filtering radius of 1.5 to smoothen the sensitivity field and use a penalty of 3.0 for density.
- The termination criteria is when the density change is less than 0.01 [4].

In addition, to trace the pareto-optimal curve via SIMP, we use two strategies:

1. **SIMP-restart**: Here, for each volume fraction, the density is initialized to a uniform density of specified volume fraction.

2. **SIMP-continuous**: Here, for each volume fraction, the density is initialized to the termination density of optimal topology of the previous volume fraction.

In the proposed method and the two strategies of SIMP, the most dominating cost is finite element analysis (FEA). Therefore, in the experiments below, we note the number of FEA runs required to reach an optimal topology, for a given volume fraction, via the proposed algorithm, and via single-objective SIMP-restart & SIMP-continuous.

5.1 Beam with Center Load

The first set of experiments is on the classic cantilevered beam-problem posed below. We assume that structures Ω must lie within a space D, illustrated in Figure 8 of unit volume, and dimensions as shown. The structure Ω is to be fixed on one edge, and must carry a unit-load F on the other end as illustrated; the material properties are $E = 1$, and $\nu = 0.3$.

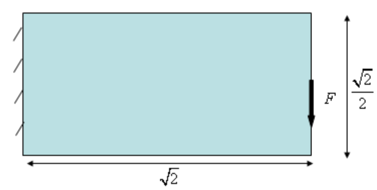

Figure 8: The cantilevered beam-problem

The table below summarizes the results for various volume fractions. For each volume fraction, we also provide: (1) the compliance as predicted by the proposed method, and that from SIMP, and (2) the total number of finite element analysis runs needed for each method. There are minor differences between the topologies generated by the two methods, but the compliances are almost identical, confirming that we have achieved pareto-optimality.

Table 1: Optimal topologies and compliances for experiment-1.

	$v = 0.9$	$v = 0.8$	$v = 0.7$	$v = 0.6$	$v = 0.5$
Proposed Method	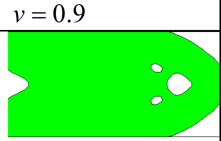 J=40.8	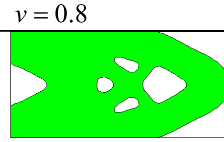 J=44	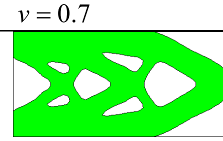 J=48.96	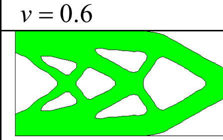 J=55.3	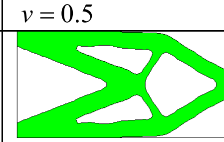 J=68

SIMP: Restart and continuous	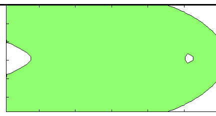 J=40.64	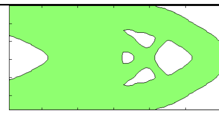 J=44	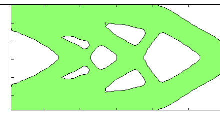 J=49.0	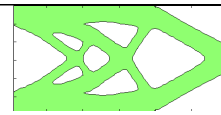 J=56.1	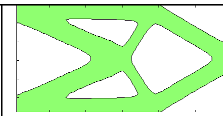 J=66.3

The figure below captures the number of *cumulative* FEA runs (the most dominating cost) for the three strategies, as a function of the volume fraction removed.

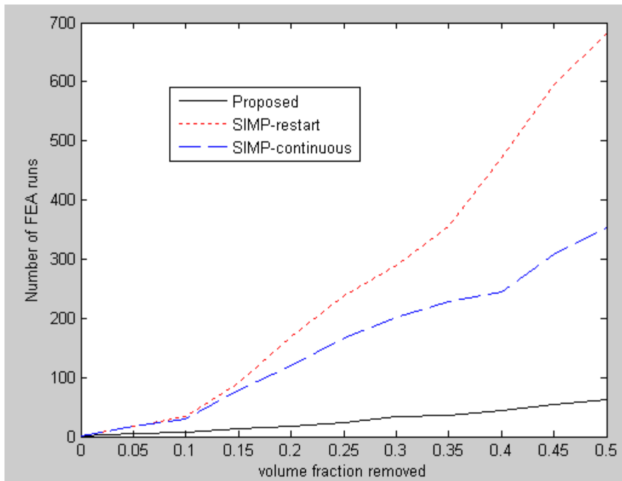

Figure 9: Number of cumulative FEA runs as a function of the volume fraction removed.

Observe that the number of FEA runs to achieve a given volume fraction for the proposed method is significantly smaller than that of either SIMP strategies. Thus, one can generate the entire set of pareto-optimal topologies with 62 FEA runs as illustrated, SIMP-restart takes 628 FEA runs, and SIMP-continuous takes 353 runs.

The figure below illustrates the pareto-optimal curve as generated by the proposed and the SIMP methods.

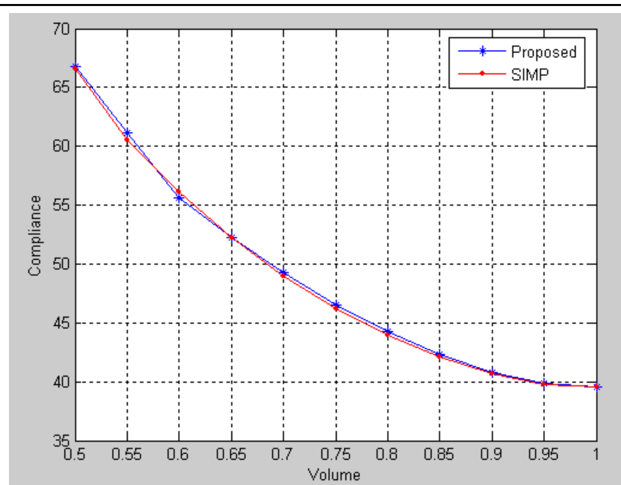

Figure 10: The pareto-optimal curve for the cantilevered beam problem.

We will now vary some of the parameters and study their impact. For example, the figure below compares the pareto-optimal curve for various mesh densities, namely (40,20), (60,30) (default), and (80,40); all other parameters being identical to the default parameters. Not surprisingly, finer density meshes yield lower pareto-optimal curves, and topologies with more ‘holes’.

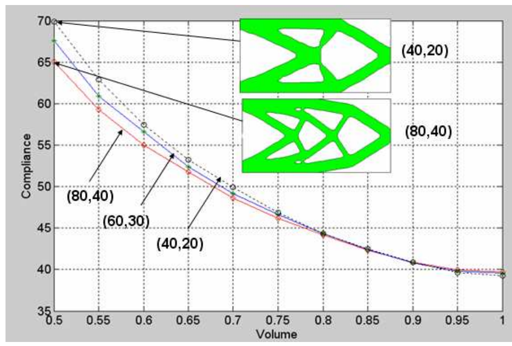

Figure 11: The pareto-optimal curves for the cantilevered beam problem for various mesh sizes.

Next we consider two additional volume step-sizes $\Delta v = 0.025$ and $\Delta v = 0.05$, and compare the pareto-optimal curves against the default $\Delta v = 0.05$; all other parameters being identical. Since the curves in Figure 12 are almost identical, we have not identified them; the topologies were also identical.

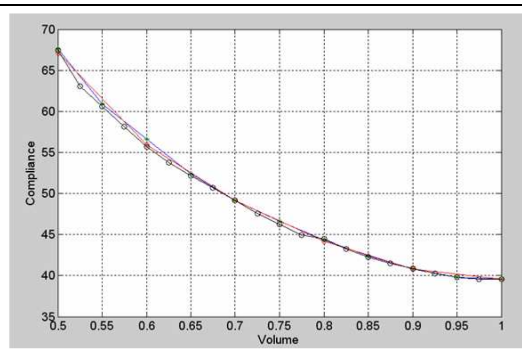

Figure 12: The pareto-optimal curves for the cantilevered beam problem for various volume step-sizes.

Finally, the pareto-optimal curve was found to be relatively insensitive to the filter radius (ranging from 0.5 to 2.0). But, for lower filter radius, topologies with larger number of holes were generated, as expected.

5.2 Beam with Tip Load

The next set of experiments is on the beam problem posed below with material parameters, etc. as before.

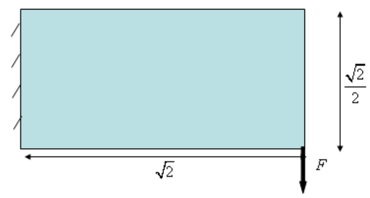

Figure 13: Experiment-2

The table below compares the results from the proposed method and SIMP for various volume fractions. Once again, there are minor differences between the topologies generated by the two methods, but the compliances are almost identical, confirming that we have achieved pareto-optimality.

Table 2: Optimal topologies and compliances for experiment-2

	$v = 0.9$	$v = 0.8$	$v = 0.7$	$v = 0.6$	$v = 0.5$
Proposed Method	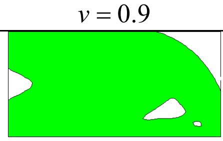 J=46.3	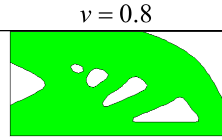 J=49.8	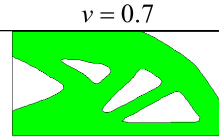 J=54.3	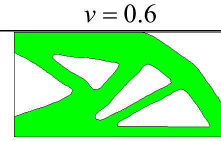 J=61.8	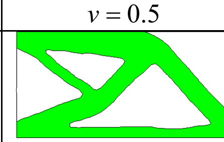 J=73.1
SIMP: Restart and continuous	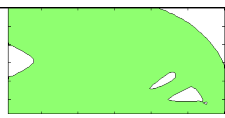 J=46.2	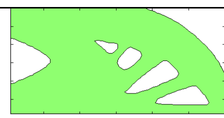 J=49.6	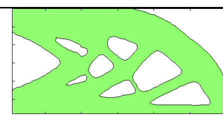 J=54.8	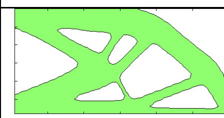 J=62.2	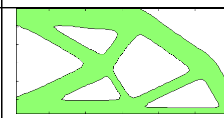 J=73

The figure below captures the number of *cumulative* FEA runs (the most dominating cost) for the three strategies, as a function of the volume fraction removed.

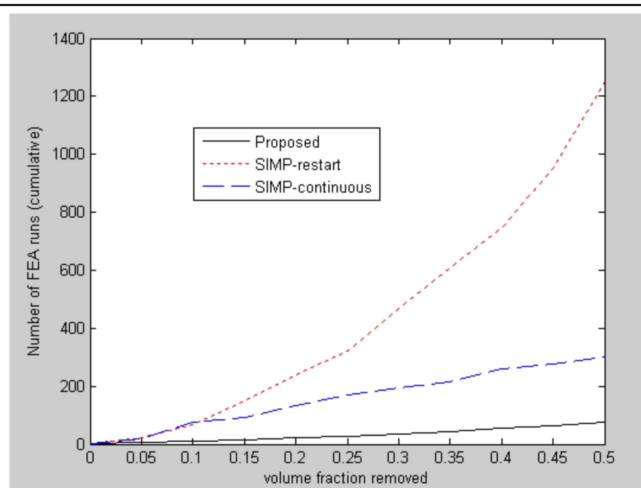

Figure 14: Number of cumulative FEA runs as a function of the volume fraction removed.

Observe that, once again, the number of FEA runs to achieve a given volume fraction for the proposed method is significantly smaller than that of either SIMP strategies. One can generate the entire set of pareto-optimal topologies with 75 FEA runs via the proposed method, while SIMP-continuous requires 250 FEA runs. The figure below illustrates the pareto-optimal curve as generated by the proposed and the SIMP methods.

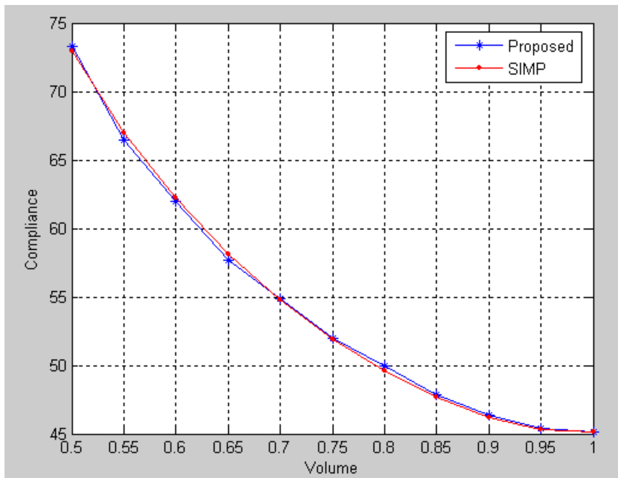

Figure 15: The pareto-optimal curve for experiment-2.

5.3 Multi-load Pareto Optimal Topologies

The theory presented in section 4 is verified through the next set of experiments. Consider the two-objective problem in Equation (4.1), where the objectives are the two compliances associated with the two load cases illustrated in Figure 7. The tables below illustrate various topologies obtained for various weight combinations, for different volume fractions.

Table 3: Optimal topologies for $v_0 = 0.75$

$w_1 = 0.2;\ \ w_2 = 0.8$	$w_1 = 0.4;\ \ w_2 = 0.6$	$w_1 = 0.5;\ \ w_2 = 0.5$	$w_1 = 0.6;\ \ w_2 = 0.4$	$w_1 = 0.8;\ \ w_2 = 0.2$
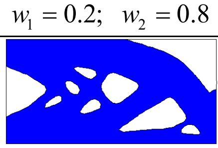 J1=52.4; J2=52.2	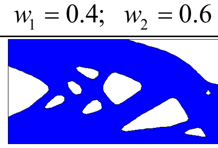 J1=49.6; J2=52.3	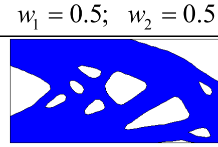 J1=48.9; J2=52.9	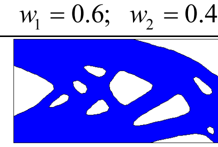 J1=47.9; J2=54.6	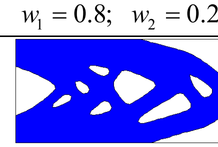 J1=47.1; J2=64.0

Table 4: Optimal topologies for $v_0 = 0.6$

$w_1 = 0.2;\ \ w_2 = 0.8$	$w_1 = 0.4;\ \ w_2 = 0.6$	$w_1 = 0.5;\ \ w_2 = 0.5$	$w_1 = 0.6;\ \ w_2 = 0.4$	$w_1 = 0.8;\ \ w_2 = 0.2$

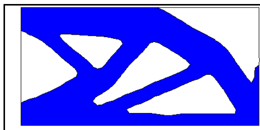 J1=70.0; J2=62.6	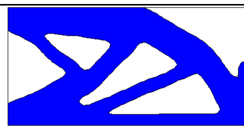 J1=76.9; J2=62.7	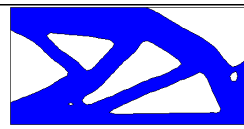 J1=63.6; J2=62.9	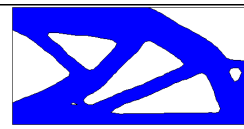 J1=62.3; J2=63.3	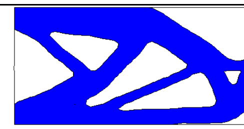 J1=61.8; J2=69.2

Figure 16 illustrates the pareto-optimal curve as generated by the proposed method in section 4 for volume fractions 0.75 and 0.6., where $J^* = w^2 J$. Further, the pareto-optimal curves for volume fraction 0.6 and the resulting topologies at $w_1 = 0.8;$ and $w_2 = 0.2;$ are illustrated in Figure 17 and Table 5.

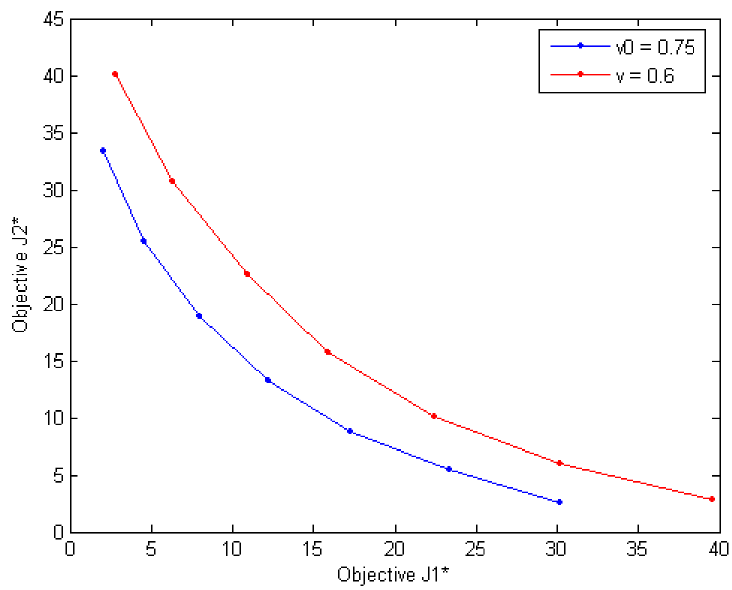

Figure 16: The pareto-optimal curves for two volume fractions.

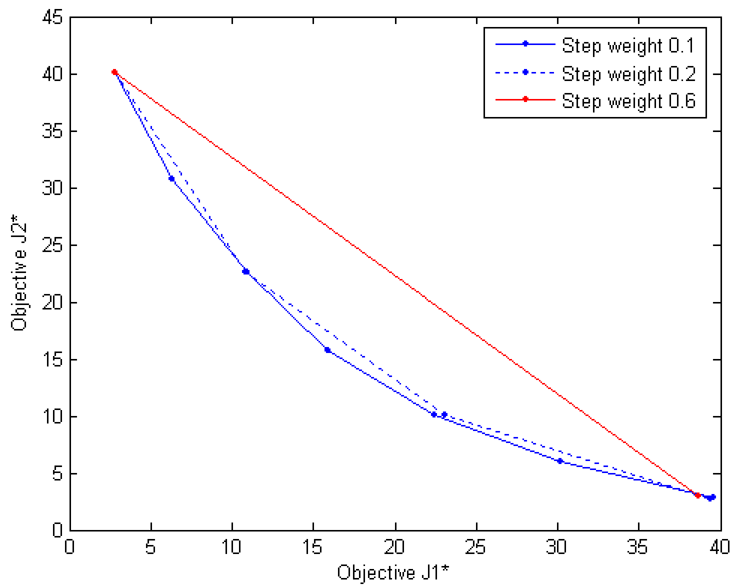

Figure 17: The pareto-optimal curves for $v_0 = 0.6$

Table 5: Resulting topologies for $v_0 = 0.6$ ($w_1 = 0.8, \ \ w_2 = 0.2$)

$\Delta w = 0.1$	$\Delta w = 0.2$	$\Delta w = 0.6$
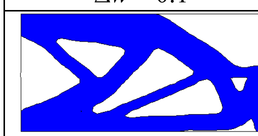 J1=61.8; J2=69.2 #FEA =53	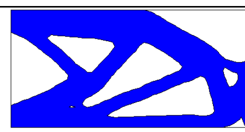 J1=61.6; J2=67.4 #FEA=41	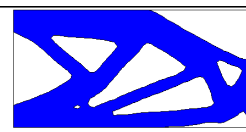 J1=60.4; J2=73.1 #FEA=44

From Figure 17 and Table 5 one can see that a larger step size can be used to reduce the computational cost without loss of accuracy. Note that #FEA iterations in Table 5 include the 35 iterations needed to converge to the desired volume fraction (domain initialization in Algorithm 3).

5.4 Tip-loaded 3-D Beam

The proposed method can be easily extended to 3-D topology optimization. The topological sensitivity expression for 3-D plane stress problems, with respect to material subtraction is given by [46]

$$\mathcal{T}^S(p) = -20\mu\sigma : \varepsilon - (3\lambda - 2\mu) tr(\sigma) tr(\varepsilon) \tag{5.1}$$

where μ and λ are the Lamé coefficients. For material addition we used the same expression, but with a negative sign.

The experiment in section 5.2 is repeated here in 3-D with the following parameters and modifications.

- The problem is illustrated in Figure 18 with $w = 48$, $d = 8$, and carrying a unit-load F.
- The domain D is discretized into unit linear hexahedral elements.
- We use a Gaussian filter of radius 1.0 to smoothen the topological sensitivity field.
- For comparison with the SIMP method, we extend the Matlab code described in [4] to 3-D with same discretization parameters.

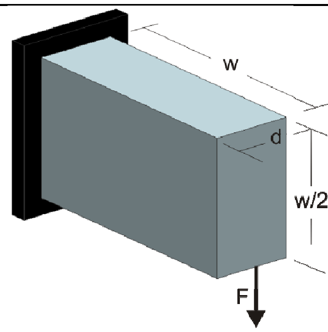

Figure 18: The 3-D tip loaded beam.

The resulting 3-D topologies at $v = 0.5$ for the proposed and the SIMP methods are shown in Figure 19.

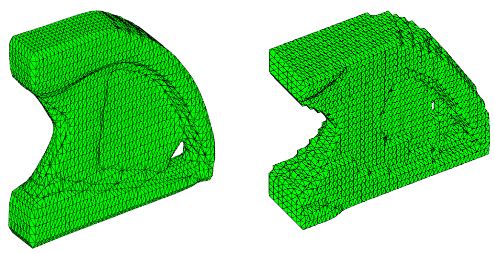

Figure 19: Optimal topologies for a volume fraction $v = 0.5$ (a) proposed method (b) SIMP.

Table 6 compares the results from the proposed method and SIMP for various volume fractions. Once again, there are minor differences between the topologies generated by the two methods, but the pareto-optimality was achieved.

Table 6: Optimal topologies for the tip-loaded 3-D beam

	$v = 0.9$	$v = 0.8$	$v = 0.7$	$v = 0.6$	$v = 0.5$
Proposed Method	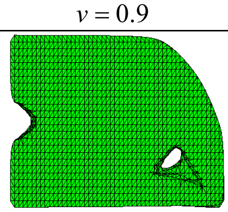 J=8.53	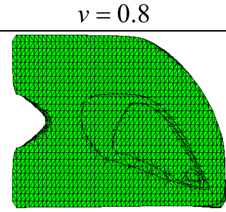 J=8.79	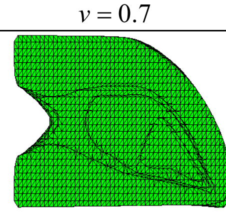 J=9.20	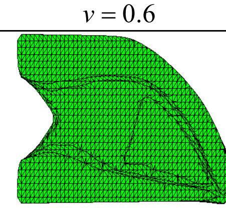 J=9.81	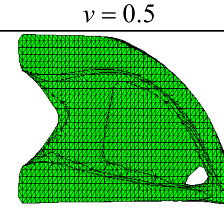 J=10.76

SIMP: (Restart & Continuous)	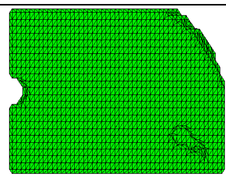 J=8.60	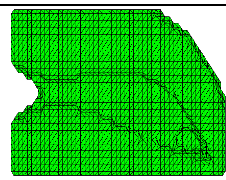 J=8.91	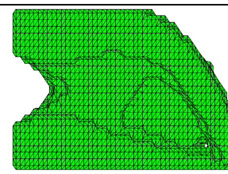 J=9.36	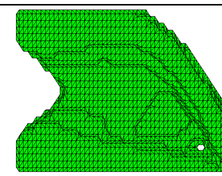 J=10.00	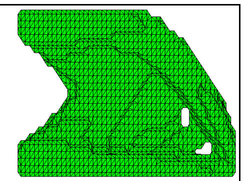 J=10.99

As before the proposed method proves to be superior to SIMP. The figure below captures the number of cumulative FEA runs (the most dominating cost) for the three strategies, as a function of the volume fraction removed.

Observe that, once again, the number of FEA runs to achieve a given volume fraction for the proposed method is significantly smaller than that of either SIMP strategies. One can generate the entire set of pareto-optimal topologies with 134 FEA runs via the proposed method, while SIMP-continuous requires 705 FEA runs.

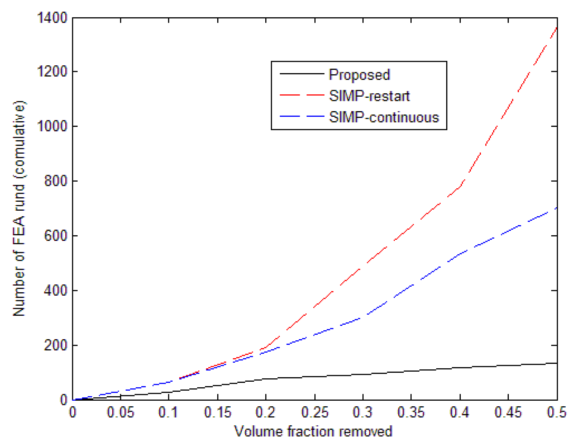

Figure 20: Number of cumulative FEA runs as a function of the volume fraction removed.

Figure 21 illustrates the pareto-optimal curve as generated by the proposed and the SIMP methods.

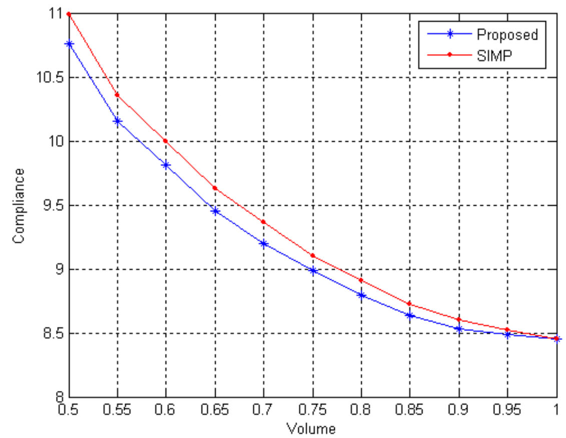

Figure 21: The pareto-optimal curve for the tip-loaded 3-D beam.

Next we explore the impact of changing the volume step size on the results. The pareto-optimal curve with $\Delta v = 0.025$, $\Delta v = 0.05$, and $\Delta v = 0.1$ is illustrated in Figure 22.

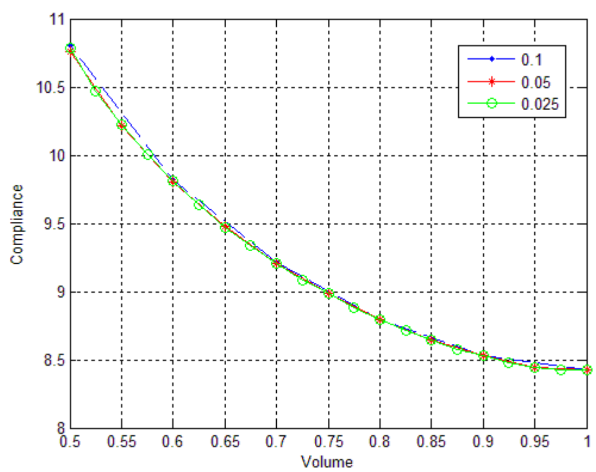

Figure 22: The pareto-optimal curves for the cantilevered beam problem for various volume step-sizes.

5.5 Cube under four point load

We emphasize the applicability of the proposed method in 3-D topology optimization with a more complex numerical example. The boundary conditions for the example are illustrated in Figure 23. The structure Ω is to be fixed on the four bottom corners, and must carry four unit-loads positioned symmetrically as shown. The material properties are E = 1, and $\nu = 0.3$; the dimension d is set to 24.

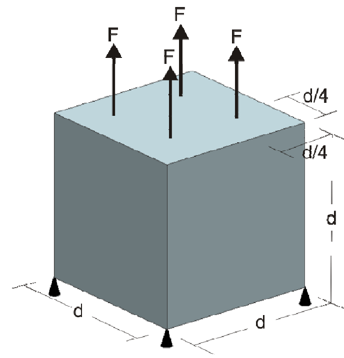

Figure 23: Cube subjected to four point loads.

The final topology at $v = 0.2$ for the proposed method and SIMP, and the pareto-optimal curve generated by the proposed method are illustrated in Figure 24 and Figure 25 respectively.

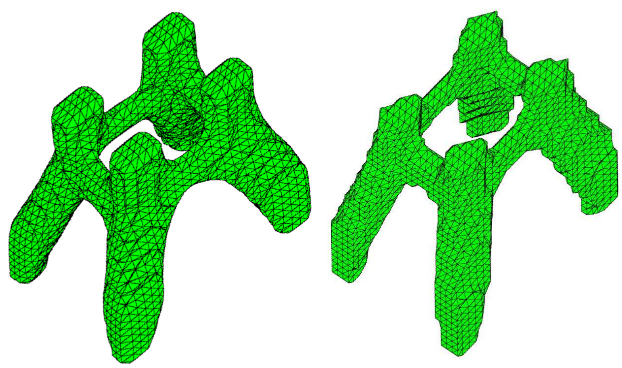

Figure 24: Optimal topologies for a volume fraction $v = 0.2$: (a) proposed method (b) SIMP.

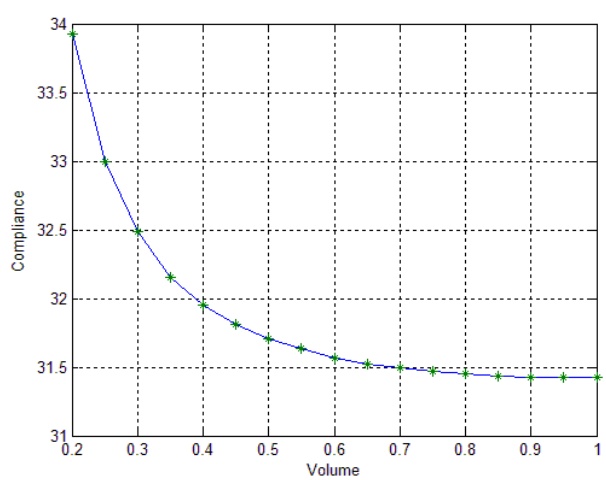

Figure 25: The pareto-optimal curve for the cube with 4 point loads.

6. CONCLUSIONS

The two most significant contributions of the paper are: (1) a theoretical framework for determining if a topology is locally pareto-optimal through an intrinsic test, and (2) an efficient algorithm for tracing pareto-optimal curves for compliance-related objectives. Future work will focus on: (a) non-compliance objectives since the topological sensitivity concept is well defined for a large class of problems, (b) higher dimension Pareto fronts, and (c) further improving the efficiency of the proposed algorithms.

7. REFERENCES

1. Bendsøe, M.P., Kikuchi, N, *Generating optimal topologies in optimal design using a homogenization method*. Computer Methods in Applied Mechanics and Engineering, 1988. 71: p. 197–224.
2. Bendsøe, M.P., *Optimal shape design as a material distribution problem*. Structural Optimization, 1989. 1(193-202).
3. Zhou, M., Rozvany, G.I.N., *The COC algorithm, part II: Topological, geometry and generalized shape optimization*. Computer Methods in Applied Mechanics and Engineering, 1991. 89: p. 197-224.
4. Sigmund, O., *A 99 line topology optimization code written in Matlab*. Structural and Multidisciplinary Optimization, 2001. 21(2): p. 120-127.
5. Allaire, G., Jouve, F., Toader, A., *Structural Optimization using Sensitivity Analysis and a Level-set Method*. Journal of Computational Physics, 2004. 194(1): p. 363-393.
6. Burger, M., Hackl, B., Ring, W., *Incorporating Topological Derivatives into Level Set Methods*. Journal of Computational Physics, 2004. 194(1): p. 344-362.
7. Wang, M.Y., Wang, X., Guo, D., *A level set method for structural topology optimization*. Computer Methods in Applied Mechanics and Engineering, 2003. 192: p. 227-246.
8. Wei, P., Wang, M. Y, *Piecewise constant level set method for structural topology optimization*. International Journal of Numerical Methods in Engineering, 2009. 78: p. 379-402.
9. Wang, M.Y., Wei, P. *Topology optimization with level set method incorporating topological derivative*. in *6th World Congress on Structural and Multidisciplinary Optimization*. 2005. Rio de Janeiro, Brazil.
10. Messac, A., Sundararaj, G.J., Tappeta, R.V., Renaud, J.E., *Ability of Objective Functions to Generate Points on Non-Convex Pareto Frontiers*. AIAA JOURNAL, 2000. 38(6): p. 1084-1091.
11. Messac, A., Ismail-Yahaya, A., *Required Relationship Between Objective Function and Pareto Frontier Orders: Practical Implications*. AIAA JOURNAL, 2001. 39(11): p. 2168-2174.
12. Cohon, J.L., *Multiobjective programming and planning*. Vol. 140. 1978, London: Academic Press, Inc.
13. Chen, T.Y., Wu, S-C, *Multiobjective optimal topology design of structures*. Computational Mechanics, 1998. 21: p. 483-492.
14. Zhang, W.H., Yang, H.C., *Efficient gradient calculation of the Pareto optimal curve in multicriteria optimization*. Structural and Multidisciplinary Optimization, 2002. 23: p. 311–319.
15. Utyuzhnikov, S.V., Maginot, J., Guenov, M.D. *Local Approximation of Pareto Surface*. in *Proceedings of the World Congress on Engineering*. 2007. London, U.K.
16. Harada, K., Sakuma, J., Kobayashi, S. *Uniform Sampling of Local Pareto-Optimal Solution Curves by Pareto Path Following and its Applications in Multi-objective GA*. in *GECCO'07, July 7–11*. 2007. London, England, United Kingdom.
17. Céa J., G., S., Guillaume, P., Masmoudi, M., *The shape and topological optimizations connection*. Computer Methods in Applied Mechanics and Engineering, 2000. 188: p. 713-726.
18. Eschenauer, H.A., Olhoff, N., *Topology optimization of continuum structures: A review*. Applied Mechanics Review, 2001. 54(4): p. 331-389.
19. Deb, K., *Multi-Objective Optimization Using Evolutionary Algorithms*. 2001, Chichester,: John Wiley & Sons,.
20. Sanchis, J., Martínez, M., Blasco, X., Salcedo, J. V., *A new perspective on multiobjective optimization by enhanced normalized normal constraint method*. Structural and Multidisciplinary Optimization, 2008. 36: p. 537–546.

21. Chen, J., Shapiro, V., Suresh, K., Tsukanov, I.,. *Parametric and Topological Control in Shape Optimization*. in *32nd Design Automation Conference*. 2006. Philadelphia: ASME.
22. Marler, R.T., Arora, J. S., *The weighted sum method for multi-objective optimization: new insights*. Structural and Multidisciplinary Optimization, 2010. 41(6).
23. Lin, J., Luo, Z., Tong, L., *A new multi-objective programming scheme for topology optimization of compliant mechanisms*. Structural and Multidisciplinary Optimization, 2010. 30: p. 241–255.
24. Luo, Z., Chen, L. Yang, J., Zhang, Y., Abdel-Malek, K., *Compliant mechanism design using multi-objective topology optimization scheme of continuum structures*. Structural and Multidisciplinary Optimization, 2005. 30: p. 142–154.
25. Das, I., Dennis, J.E., *A closer look at drawbacks of minimizing weighted sums of objectives for Pareto set generation in multicriteria optimization problems*. Structural Optimization, 1997. 14: p. 63-69.
26. Hamda, H., Roudenko, O., Schoenauer, M. *Application of a multi-objective evolutionary algorithm to topology optimum design*. in *Fifth International Conference on Adaptive Computing in Design and Manufacture*. 2002.
27. Madeira, J.F.A., Rodrigues, H., Pina, H., *Multi-objective optimization of structures topology by genetic algorithms*. Advances in Engineering Software, 2005. 36: p. 21-28.
28. Padhye, N. *Topology Optimization of Compliant Mechanism using Multi-Objective Particle SwarmOptimization*. in *GECCO’08, July 12–16*. 2008. Atlanta, Georgia, USA.: ACM.
29. Chen, T.-Y., Wu, S.-C., *Multiobjective optimal topology design of structures*. Computational Mechanics, 2002. 21: p. 483-492.
30. Zienkiewicz, O.C., Taylor, R. L., *The Finite Element Method for Solid and Structural Mechanics*. 6th ed. 2005: Elsevier.
31. Nocedal, J., Wright, S.J., *Numerical optimization*. 2 ed. Springer Series in Operations Research. 2006, New York: Springer Science + Business Media.
32. Eschenauer, H.A., Kobelev, V. V., Schumacher, A, *Bubble method for topology and shape optimization of structures*. Structural Optimization, 1994. 8: p. 42-51.
33. Feijóo, R.A., Novotny, A. A., Taroco, E., Padra, C., *The Topological Derivative for the Poisson's Problem*. Mathematical Models and Methods in Applied Sciences, 2003. 13(12): p. 1825-1844.
34. Novotny, A.A., Feijóo, R. A., Taroco, E., Padra, C., *Topological-Shape Sensitivity Analysis*. Computer Methods in Applied Mechanics and Engineering, 2003. 192(7): p. 803-829.
35. Novotny, A.A., Feijóo, R. A., Taroco, E., Padra, C. *Topological Sensitivity Analysis for Three-dimensional Linear Elasticity Problem*. in *6th World Congress on Structural and Multidisciplinary Optimization*. 2005. Rio de Janeiro.
36. Novotny, A.A., Feijóo, R. A., Taroco, E., Padra, C., *Topological-Shape Sensitivity Method: Theory and Applications*. Solid Mechanics and its Applications, 2006. 137: p. 469-478.
37. Belytschko, T., Xiao, S. P., Parimi, C., *Topology Optimization with Implicit Functions and Regularization*. International Journal for Numerical Methods in Engineering, 2003. 57(8): p. 1177–1196.
38. Sokolowski, J., Zochowski, A., *On Topological Derivative in Shape Optimization*. SIAM journal on control and optimization, 1999. 37(4): p. 1251-1272.
39. Sokolowski, J., Zochowski, A., *Optimality Conditions for Simultaneous Topology and Shape Optimization*. SIAM journal on control and optimization, 2003. 42(4): p. 1198-1221.
40. Samet, B., *The topological asymptotic with respect to a singular boundary perturbation*. Comptes Rendus Mathematique, 2003. 336(12): p. 1033-1038.
41. Dambrine, M., Vial, G., *Influence of a boundary perforation on the Dirichlet energy*. Control and Cybernetics, 2005. 34(1): p. 117-136.
42. Gopalakrishnan, S.H., Suresh, K.,, *Feature Sensitivity: A Generalization of Topological Sensitivity*. Finite Elements in Analysis and Design, 2008. 44(11): p. 696-704.
43. Feijóo, R.A., Novotny, A.A., Taroco,E., Padra, C., *The topological-shape sensitivity method in two-dimensional linear elasticity topology design*, in *Applications of Computational Mechanics in Structures and Fluids*, V.S. S.R. Idelsohn, Editor. 2005, CIMNE.
44. Amstutz, S., *Sensitivity analysis with respect to a local perturbation of the material property*. Asymptotic Analysis, 2006. 49(1-2): p. 87-108.
45. Norato, J.A., Bendsøe, M. P., Haber, R.B., Tortorelli, D.A., *A topological derivative method for topology optimization*. Structural and Multidisciplinary Optimization, 2007. 33: p. 375–386.
46. Garreau. S., G., Ph., Masmoudi, M., *The Topological Asymptotic for PDE Systems: The Elasticity Case*. SIAM Journal on Control and Optimization, 200. 39(6): p. 1756-1778.